Supplementary Material for NeILF

In this supplementary material, we show implementation details and additional results of the proposed method. For relighting results, please refer to our **supplementary video**.

1 Implementation Details

1.1 Network Architecture

The detailed architecture of the proposed method is shown in Fig. 1. The overall design of our network is simple yet effective. We believe the architecture can be easily re-implemented or extended by other researchers.

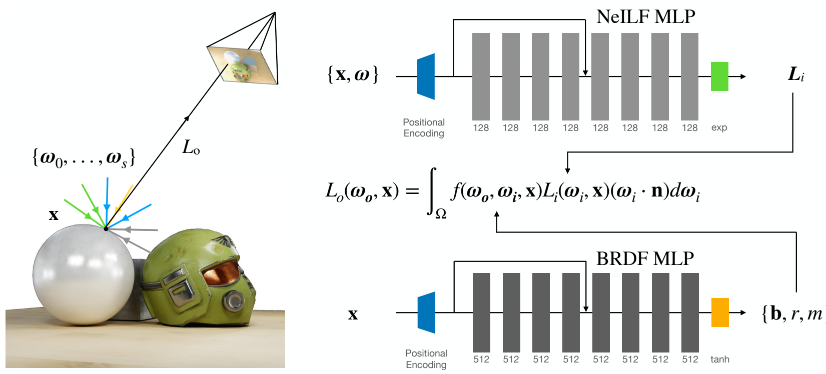

Fig. 1: Network architecture of the proposed NeILF.

1.2 Detailed BRDF Functions

In this section, we describe detailed implementations of our normal distribution term D, Fresnel term F, and geometry term G. The normal distribution function D is approximated by the Spherical Gaussian function:

$$D(\mathbf{h}; r) = S(\mathbf{h}, \frac{1}{\pi r^2}, \mathbf{n}, \frac{2}{r^2}) = \frac{1}{\pi r^2} e^{\frac{2}{r^2}(\mathbf{h}\cdot\mathbf{n}-1)}.$$

The Fresnel term is given as:

$$F(\boldsymbol{\omega}_o, \mathbf{h}; \mathbf{b}, m) = F_0 + (1 - F_0)(1 - (\boldsymbol{\omega}_o \cdot \mathbf{h})^5),$$
$$\text{where } F_0 = 0.04(1 - m) + \mathbf{b}m.$$

Finally, the geometry term is approximated by the GGX function [2]:

$$G(\boldsymbol{\omega}_i, \boldsymbol{\omega}_o, \mathbf{n}; r) = G_{GGX}(\boldsymbol{\omega}_i \cdot \mathbf{n}) G_{GGX}(\boldsymbol{\omega}_o \cdot \mathbf{n}),$$
$$\text{where } G_{GGX}(z) = \frac{2z}{z + \sqrt{r^2 + (1 - r^2)z^2}}.$$

2 Synthetic Dataset

2.1 Dataset Setup

In this section, we illustrate the camera and lighting setup of our in-house synthetic dataset. The camera trajectory is shown in Fig. 2, which contains 96 camera positions with the outside-look-in trajectory. The mixed lighting set up is also shown in Fig. 2, which consists of two near-range point lights, two near-range area lights and one background environment map from {*Env-city*, *Env-studio*, *Env-castel*} (see main paper Sec. 5.2 for details).

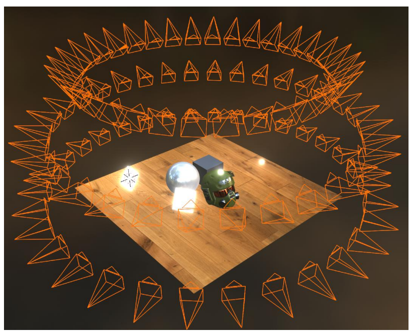

Fig. 2: The camera and the near-range light setting of our synthetic dataset. We add two point lights and two area lights in the mixed lighting to lit the scene.

Fig. 3: Two selected points for incident light visualization. Estimated incident lights for $\mathbf{x}_1$ and $\mathbf{x}_2$ are visualized in Fig. 4

2.2 Lighting Estimation

Due to the space limit, we did not analyze the lighting estimation result in the main paper. In this section, we demonstrate the powerful capability of the proposed NeILF for lighting modelling. As shown in Fig. 3, we select two surface points on top of the helmet and the cube to show the estimated incident lights at these two points. The lighting estimation results under six lighting conditions are visualized in Fig. 4. Our lighting estimations enjoy the following properties:

- For environment map based lightings (*Env-city*, *Env-studio* and *Env-studio*), our incident light estimations successfully recovery corresponding environment maps at both points.
- For mixed lightings (*Mix-city*, *Mix-studio* and *Mix-studio*), our results well explain all light sources, including background environment maps, two near-range point lights, and two near-range area lights.
- For mixed lightings, we generate consistent point and area light estimations (high lights in images) across different background environments.

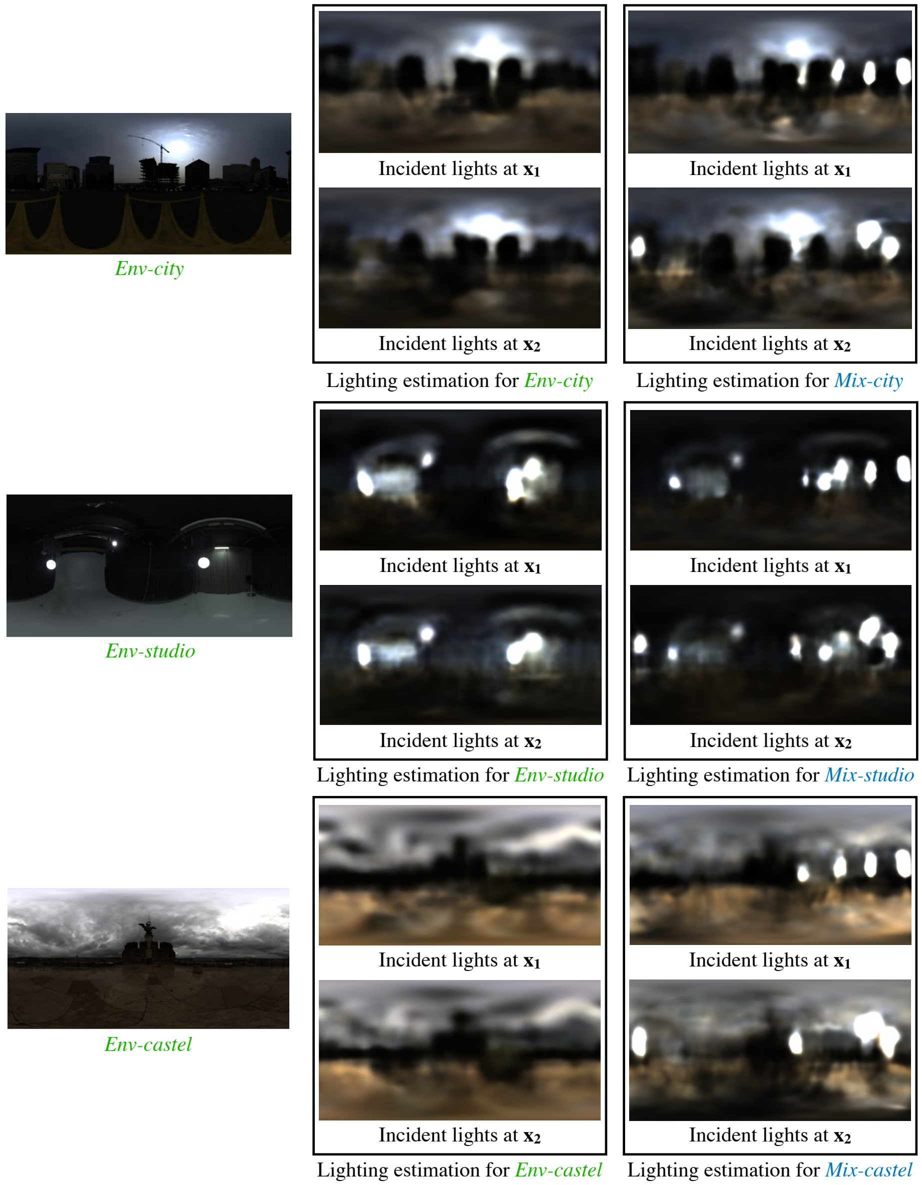

Fig. 4: Visualizations of our lighting estimations. For environment map based lightings (*Env-city*, *Env-studio* and *Env-studio*), our incident light estimations correctly recovery GT environment maps at both points (see Fig. 3). For mixed lightings with point and area lights (*Mix-city*, *Mix-studio* and *Mix-studio*), our results well explain all light sources. Note that the three mixed lightings share the same near-range light settings as shown in Fig. 2, and we are able to generate consistent point and area light estimations (high lights in images) across different background environments.

2.3 Ablation Study on Input Geometry Quality

We further analyze how input mesh quality would affect our predictions. For synthetic objects, we randomly perturb the mesh vertex with $d \in [-\delta, \delta]$ along its normal to simulate noisy meshes at two different levels ($\delta = \{\frac{1}{256}, \frac{1}{128}\}$). For reference, the size of the cube is $2 \times 2 \times 2$. From Table 1 and the Fig. 5 we find that the rendering quality will drop and the noisy base color will occur, which we believe are mainly caused by the inaccurate surface normal used in rendering.

Table 1: The influence of the input geometry quality.

	Env-city	Env-studio	Env-castel	Mix-city	Mix-studio	Mix-castel
NeILF	33.77	31.07	35.28	31.11	28.59	32.11
delta=1/256	31.93	29.96	33.73	29.74	27.82	30.47
delta=1/128	30.29	29.38	32.64	29.11	27.39	28.93

Fig. 5: The influence of the input geometry quality.

3 DTU and BlendedMVS Datasets

We show BRDF estimation of all DTU [1] scenes in Fig. 6 and all BlendedMVS [3] scenes in Fig. 7.

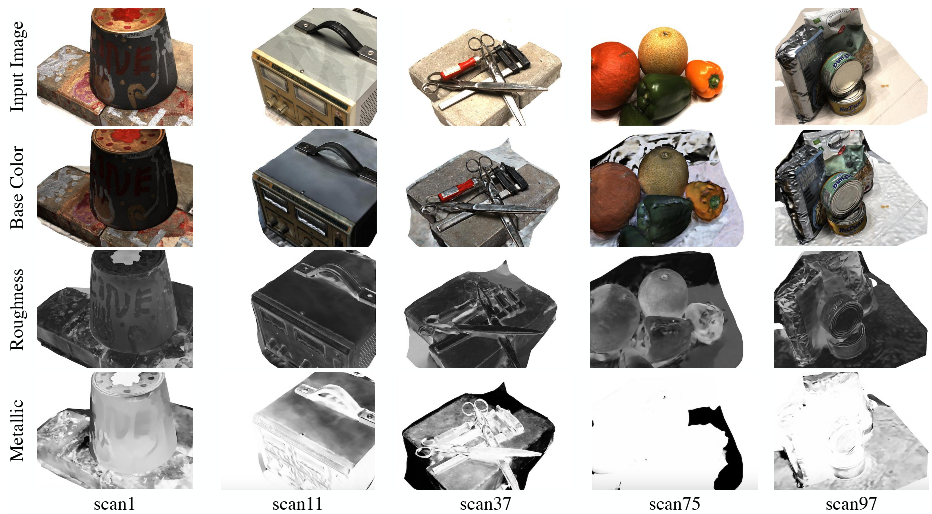

Fig. 6: Results of DTU [1] scenes.

Fig. 7: Results of BlendedMVS [3] scenes.

4 Relighting

In this section, we show the relighting result of our BRDF estimation. Given a mesh geometry input, we apply the the Iso-charts[4] algorithm to parameterize the mesh surface as a 2D UV map. Then, for each pixel in the UV map, we pass the corresponding surface point to the BRDF MLP to obtain its BRDF values. The resulting BRDF texture maps (Fig. 8) can be directly used in rendering pipelines for relighting. Please refer to our **supplementary video** for convincing results.

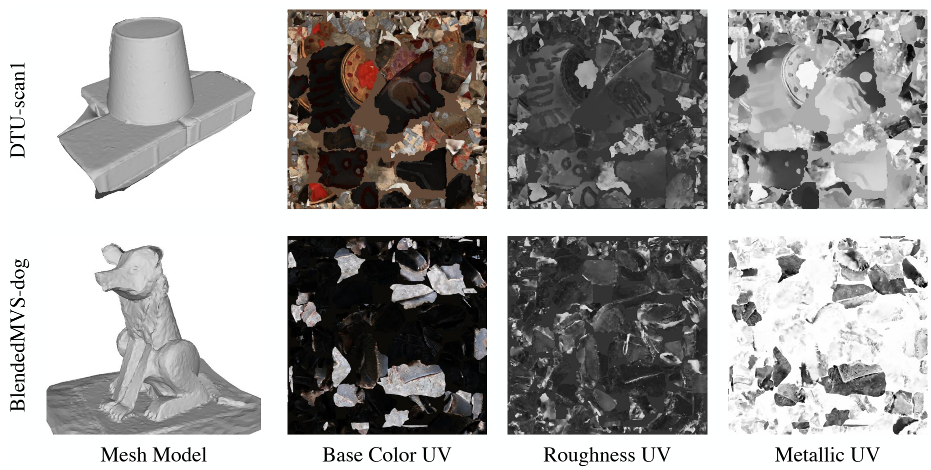

Fig. 8: Exported BRDF UV maps.

Bibliography

[1] Jensen, R., Dahl, A., Vogiatzis, G., Tola, E., Aanæs, H.: Large scale multi-view stereopsis evaluation. In: CVPR (2014)

[2] Walter, B., Marschner, S., Li, H., Torrance, K.: Microfacet models for refraction through rough surfaces. In: EGSR (2007)

[3] Yao, Y., Luo, Z., Li, S., Zhang, J., Ren, Y., Zhou, L., Fang, T., Quan, L.: Blendedmvs: A large-scale dataset for generalized multi-view stereo networks. In: CVPR (2020)

[4] Zhou, K., Synder, J., Guo, B., Shum, H.Y.: Iso-charts: stretch-driven mesh parameterization using spectral analysis. In: Proceedings of the 2004 Eurographics/ACM SIGGRAPH symposium on Geometry processing (2004)